Effects of Nozzle Exit Geometry on Forebody Vortex Control Using Blowing

Nathan M. Gittner* and Ndaona Chokani†

North Carolina State University, Raleigh, North Carolina 27695

An experimental study has been undertaken to examine the influence of the blowing nozzle exit geometry on the effectiveness of the aft blowing technique for forebody vortex control. The experiments were conducted with a 3.0-caliber tangent ogive model at subsonic velocities and a Reynolds number of 8.4×10^4 based on the model diameter. Asymmetric aft blowing was accomplished using both a single nozzle and a double nozzle configuration. Detailed surface pressure measurements on the model were obtained and local side forces determined. The experimental results show that both the height and the width of the blowing nozzle exit geometry are important parameters that determine the effectiveness of aft blowing; a broad, low-positioned blowing nozzle exit geometry is found to be most effective for the forebody vortex control technique using aft blowing.

Nomenclature

A_{ref} = reference area, model base area, 62.2 cm^2
C_p = pressure coefficient, $(p - p_\infty)/q_\infty$
C_y = sectional side force coefficient, based on unit radius and unit length, $\Sigma\, 2\pi C_p \sin \phi$
C_μ = blowing coefficient, $(\dot{m}_j u_j)/(q_\infty A_{ref})$
D = base diameter of the model, 8.9 cm
d = local diameter of the model
$\dot{m}_j$ = mass flow rate through the blowing nozzle
p = local static pressure
p_∞ = freestream static pressure
q_∞ = freestream dynamic pressure
u_j = exit velocity from the blowing nozzle
x = axial distance from model apex
$\bar{y}$ = distance from the surface of the model to the geometric center of the nozzle exit
z_{max} = maximum width of the nozzle exit
α = angle of attack
ΔC_y = incremental change in sectional side force coefficient, C_y (blowing) $- C_y$ (no blowing)
ϕ = azimuthal location from windward meridian
ϕ_b = azimuthal location of the nonblowing nozzle from the windward meridian
ϕ_j = azimuthal location of the blowing nozzle from the windward meridian

Introduction

THE flowfield around the forebody of an aircraft at high angles of attack is dominated by the system of vortices which are formed and separate asymmetrically. This asymmetric vortex configuration produces side forces and yawing moments that can render the control of the aircraft difficult or even impossible. This problem is compounded at the higher angles of attack due to the fact that the conventional control surfaces (vertical and horizontal stabilizers) are washed out by the wake of the fuselage and wings. The combat agility requirements of present and future generation high-performance aircraft dictate the need for controlled flight at high

*Graduate Research Assistant, Department of Mechanical and Aerospace Engineering. Student Member AIAA.
†Associate Professor, Department of Mechanical and Aerospace Engineering. Member AIAA.

angles of attack, and thus there is a strong motivation to control the forebody vortex asymmetry in this flight regime.[1]

Previous work[2] has shown that the forebody vortex asymmetry is produced by small imperfections at the tip of the forebody and out-of-roundness of the model tip region due to imperfections in the machining process. It was also shown that blunting the nose of a body was effective in decreasing the vortex asymmetry.[3] This was due to the fact that when a perturbation is positioned in the near tip region of a body, the ratio of the perturbation height to the local radius of the body was smaller for a blunted body than a pointed one, and the perturbation had a smaller effect on the forebody vortices. The forebody vortices could be positioned to a desired pattern with the addition of discrete surface perturbations at various locations on the near tip region of a slender body. When the nose tip geometry was altered, namely the circular cross section was machined to an elliptic cross section, a regular, repeatable, and predictable behavior of the forebody vortices was observed.[4] These results provided an improved understanding of forebody vortex management techniques using geometric methods.

More recently, a number of research studies have been conducted to develop pneumatic techniques of controlling the asymmetric forebody vortices in order to manage the forces and moments acting on the aircraft. Aft blowing has emerged as one such promising technique. Previous research in the area of aft blowing has shown that 1) the optimal axial location of the jet blowing is as close to the forebody apex as possible, since then jet blowing can most influence the flow separation and the strong interaction between the vortices; 2) the angular location of the aft blowing nozzle is found to be optimal in the range of 120–150 deg, measured from the windward generator; and 3) the baseline system of vortices determines the effectiveness of vortex control by jet blowing. Namely, the jet blowing is more effective for control of the forebody vortex system if the baseline flowfield has only a small degree of asymmetry.[5-8] In recent work a control mechanism has been proposed[6] for vortex control by jet blowing (Fig. 1). Once blowing is initiated on the leeward side of the body, the jet entrainment moves the blowing-side separation leeward; the vortex on the blowing side moves lower, and the nonblowing-side vortex moves higher while the separation on the nonblowing side moves windward. Based on this flow model, jet blowing functions primarily to control the flow separation by entrainment.

The primary objective of this study was to determine if the blowing nozzle exit geometry was an important parameter in optimizing the effectiveness of aft blowing. In previous studies
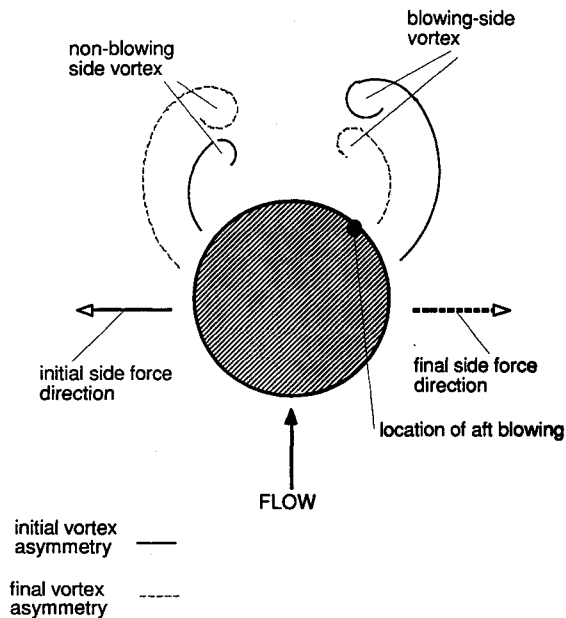
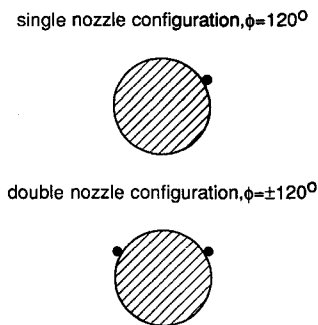Fig. 1 Proposed control mechanism—forebody vortex control by jet blowing.

Fig. 2 Nozzle configurations (pilot's view).

the nozzle exit cross section has been either circular[5,7,8] or elliptical.[6] It may be expected that a nozzle exit cross section with a geometric center closer to the surface may be more effective in influencing the flow separation than a nozzle exit with a relatively higher geometric center. On the other hand, practical considerations, such as the difficulty of fabricating minute submerged nozzles, may limit the proximity to the surface with which the blowing nozzle may be placed; thus it is of interest to assess the effectiveness of aft blowing with various nozzle exit cross sections. In addition, an improved knowledge of the effects of the nozzle exit geometry on the effectiveness of aft blowing will lead to a better understanding of the detailed mechanisms associated with the flow entrainment of this forebody vortex control technique. In the tests reported here, the first phase of the study was conducted with a single nozzle positioned on the forebody model at ϕ_j = 120 deg, that is on the port side from the pilot's view (Fig. 2a). The baseline test conditions were determined for this configuration with no blowing, and then the effect of blowing from different nozzle exit geometries examined. As discussed above, the baseline vortex system is also important in determining the blowing effectiveness, since the presence of the nozzle is itself a geometric perturbation. Therefore, in the second phase of the study a symmetrically positioned nozzle was also placed on the model at ϕ_h = 240 deg, that is on the starboard side from the pilot's view, in addition to the blowing nozzle; this is termed here as the double nozzle configuration (Fig. 2b). The no blowing case of this configuration was used as the baseline condition in the second phase of the study. For both the single and double nozzle configurations, the

effects of the angle of attack and the nozzle exit geometry were examined.

Experimental Procedure

The experiments were conducted in the North Carolina State University Subsonic Wind Tunnel. The tunnel test section is 0.81 m high × 1.14 m wide × 1.17 m long, and equipped with Plexiglas® sides and top. The test model used to represent the forebody of an aircraft was a 3.0-caliber tangent ogive body equipped with a cylindrical afterbody and interchangeable nose tips (Fig. 3). The model was instrumented with three circumferential rows of pressure taps which are referred to in this article as rows 1, 2, and 3, from the most upstream row. The angular tap spacing was 15 deg at rows 1 and 2, and 10 deg at row 3. The hollow model was rigidly mounted on a sting. Dried, pressurized air was supplied from an external source, routed along the sting, through the base of the model, and into a plenum chamber which was firmly fitted within the model. A very short length of tygon tubing supplied the air from the plenum chamber to the blowing nozzles.

The blowing nozzles were positioned on the interchangeable nose tips (Fig. 4). Five different blowing nozzle exit geometries were examined in this study. These nozzles and their exit geometry dimensions are shown in Table 1. The nozzle exit cross-sectional areas were the same for all blowing nozzles, but the shapes of the cross-sectional areas were different to represent the following: 1) a semiellipse with horizontal major axis, 2) a semicircle with horizontal major axis, 3) an ellipse with horizontal major axis, 4) a semiellipse with horizontal minor axis, and 5) a circle. The numerals are used to reference the blowing nozzles in this article and indicate an ascending geometric mean height. The geometric mean height $\bar{y}/d$ of the nozzles is shown in Table 1 and is used in this study to provide a measure of the effective height of the jet exiting from the nozzle. The effective width of the jets is characterized by the maximum horizontal dimension z_{max}/d, which is also shown in Table 1. All nozzles had the same exterior geometry of 0.25 cm high × 0.44 cm wide × 0.51 cm long. The nozzles were positioned on individual nose tips and located at ϕ_j = 120 deg for the tests reported in this article. The jets were directed tangential to the model surface, and the nozzle exit plane set at x/D = 0.125, where d is 0.95 cm. For some tests a blank nozzle of same exterior dimensions
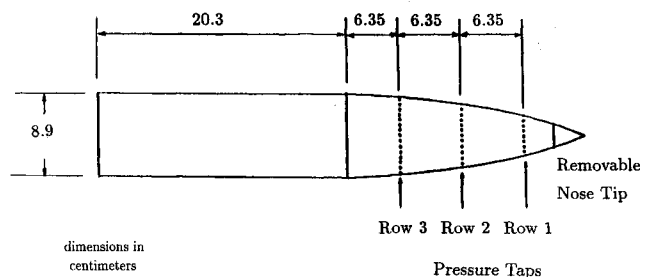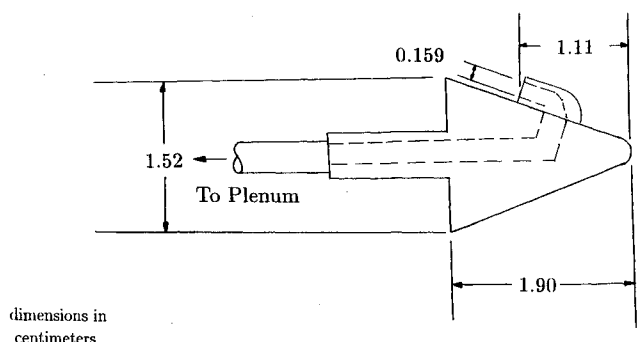

Fig. 3 3.0-caliber tangent-ogive model.

Fig. 4 Removable nose tip with blowing nozzle.

Table 1 Blowing nozzle specifications

Blowing nozzle	Exit geometries	$\bar{y}/d$	z_{max}/d
1		0.0354	0.334
2		0.0499	0.235
3		0.0588	0.235
4		0.0627	0.167
5		0.0836	0.167

was glued at a symmetric position with respect to the windward generator, $\phi_b = 240$ deg, to reduce the asymmetry in the baseline flow. Prior to the wind-tunnel testing, the blowing nozzles were calibrated to determine C_μ. The apparatus used to calibrate the blowing nozzles included a flow meter placed in-line between the plenum chamber and the blowing nozzle, a Statham pressure transducer (100 psia), and dried air supply. The tube lengths were the same during the nozzle calibrations and the subsequent wind-tunnel testing. The pressure drop across the flow meter was measured and observed to be negligible. The volumetric flow rate and the plenum stagnation pressure and temperature were measured and used to determine C_μ. The procedure is described in detail in Ref. 9.

Flow visualization was accomplished using a tufted grid technique. The grid measured 34.5 cm on a side and was constructed to be placed around half of the model while being supported independent of the model. The location of the grid during testing was $x/D = 3.79$ with the grid being positioned normal to the model surface. The tufts were spaced 2.8-cm apart and consisted of a 2.5-cm cotton thread fastened to the wire grid at one end and to the 5.0-cm cotton tuft at the other end. Cross-sectional photographs were taken looking down the axis of the forebody model.

The pressures were measured by a pair of Validyne differential transducers (± 8.89 cm of water) connected to a pair of 48-port Scanivalve modules and a Hewlett-Packard 9122 computer. The sting position was also computer controlled, and the angle of attack varied in 10-deg increments from 40 to 60 deg, with no sideslip. The blowing coefficients examined were 0.0 and 0.4 for all nozzles. All testing was performed at a freestream velocity of 13.7 m/s, which corresponded to a laminar Reynolds number of 8.4×10^4, based on the forebody model base diameter.

Results and Discussion

Single Nozzle Configuration

Figure 5 shows the pressure coefficient distributions for the baseline test condition. The trends observed with blowing nozzle 5 are presented as a representative case. The blowing nozzle was sealed, $C_\mu = 0$, while the angle of attack was increased from 40 to 60 deg in 10-deg increments. When the
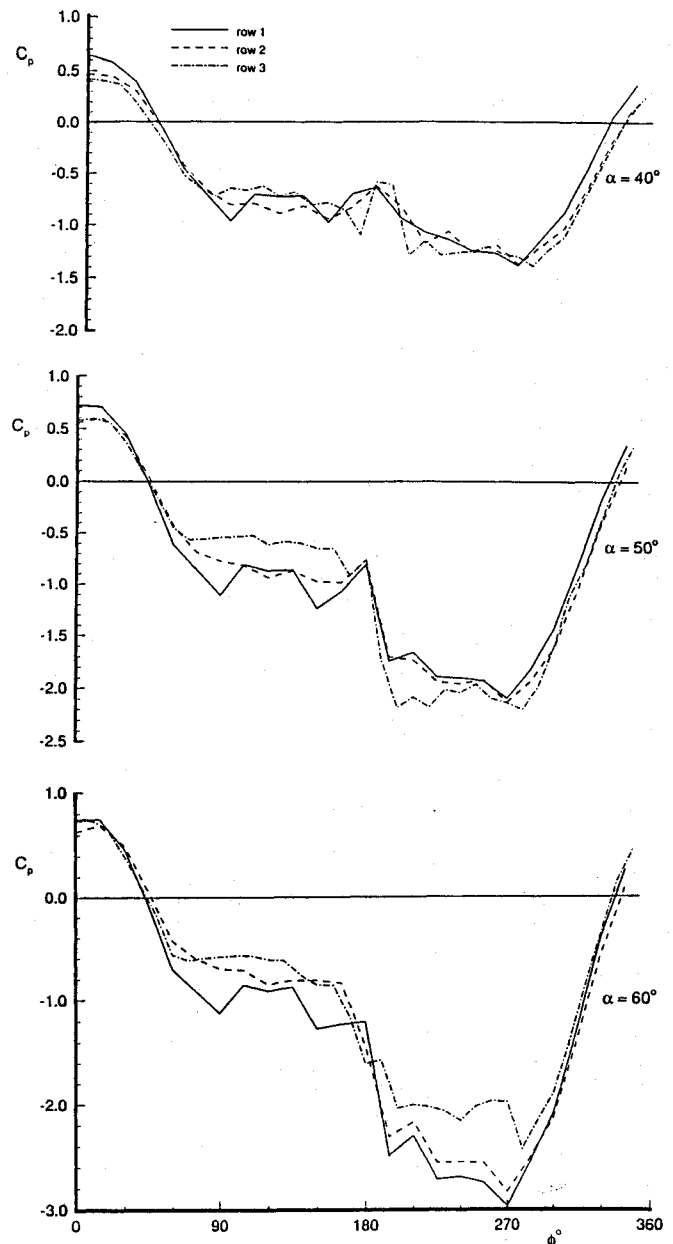

Fig. 5 Pressure coefficient for single nozzle configuration baseline condition for nozzle 5, $C_\mu = 0.0$.

model was positioned at 40-deg angle of attack, a slight vortex asymmetry was observed. On the port side of the body the vortex has assumed a "high" position, and on the starboard side the vortex has assumed a "low" position. This is inferred from the more positive C_p in the range 90 deg $\leq \phi \leq$ 180 deg, compared with the C_p in the range 180 deg $\leq \phi \leq$ 270 deg, which are more negative. At 50-deg angle of attack the vortex asymmetry was much greater. At $\alpha = 60$ deg, still greater vortex asymmetries were observed. These preliminary pressure measurements verified that an increasing degree of flow asymmetry is observed as the angle of attack is increased. These asymmetric vortex flowfields, with no-blowing, observed at all three angles of attack tested, will be used as the "baseline" conditions for the single nozzle configuration.

Figure 6 shows the baseline sectional side forces for all nozzle exit geometries plotted against the mean geometric center of the blowing nozzle exit plane, $\bar{y}/d$. It is observed that the variation of the sectional side force of each row at a given angle of attack is small. This small variation shows that the effects of interchanging the blowing nozzles resulted in only small differences in the flowfield, and that the baseline
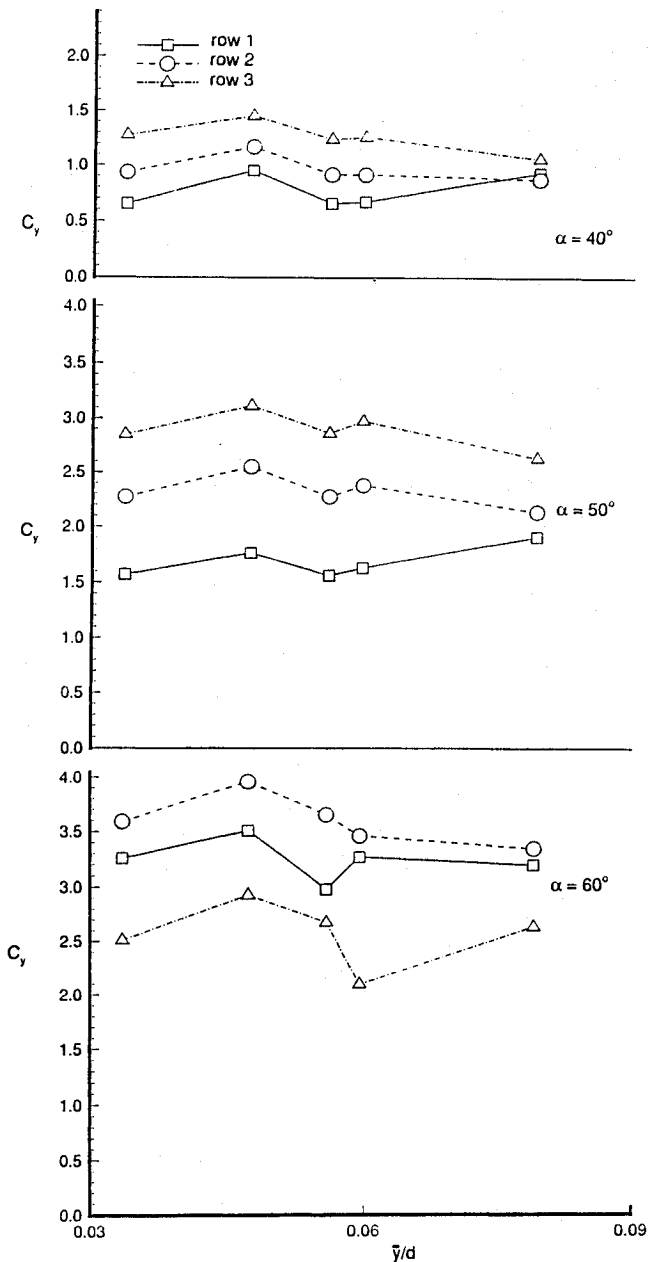
Fig. 6 Sectional side force coefficient for single nozzle configuration baseline condition, $C_\mu = 0.0$.
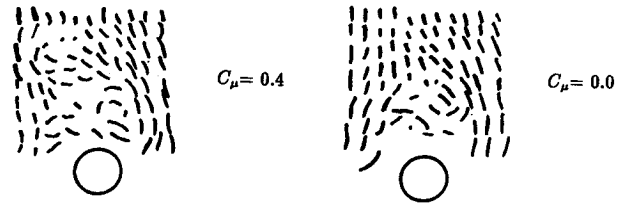

Fig. 7 Cross-sectional flow visualization: wool tuft pattern for nozzle 1 at $\alpha = 50$ deg, $C_\mu = 0.0$ and 0.4 (pilot's view).

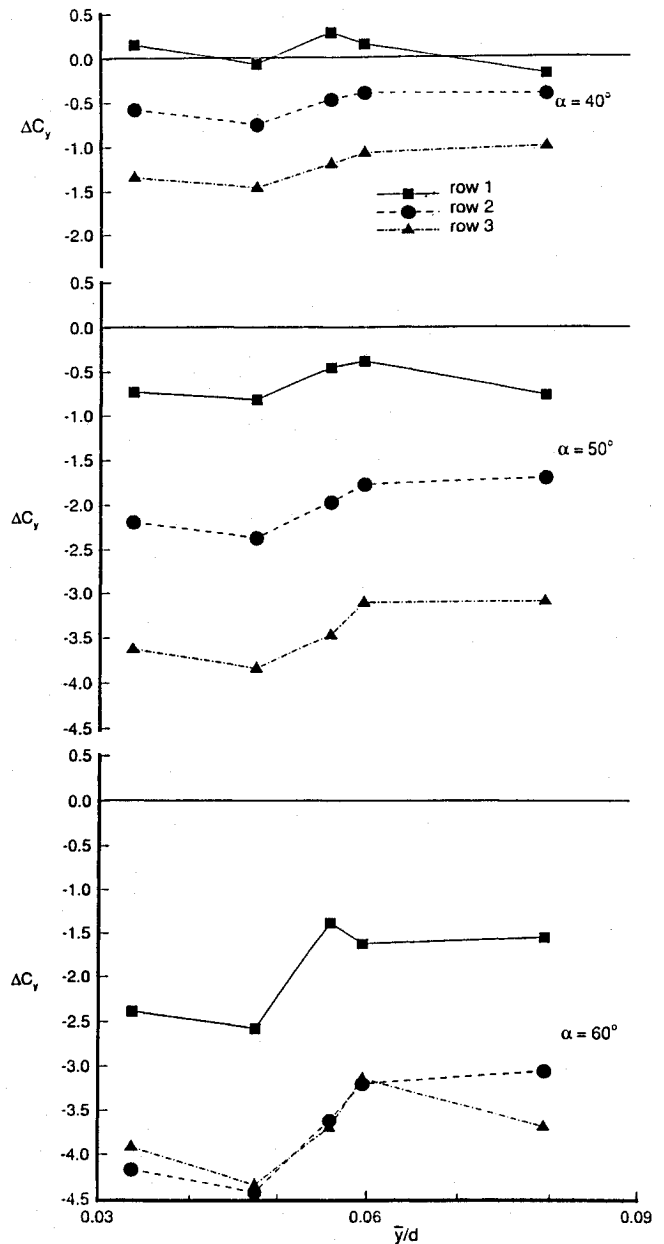Fig. 8 Incremental sectional side force coefficient for single nozzle configuration baseline condition, $C_\mu = 0.4$.

conditions for the five blowing nozzles were all quite similar. (As will be discussed later, the effect of blowing from each nozzle exit is marked, different, and identifiable.) The positive C_y indicates a side force directed towards starboard, and C_y increases in magnitude as the angle of attack is increased. This confirmed the previous observations in the baseline pressure coefficient distributions.

The effect of blowing is first observed from some typical flow visualization results presented in Fig. 7. Shown are the results from nozzle 1 blowing at $C_\mu = 0$ and 0.4, and the model positioned at $\alpha = 50$ deg. The flow visualization view is also shown from the pilot's view. The baseline conditions produced a vortex asymmetry with the starboard vortex (that is, the vortex on the no blowing-nozzle-side) positioned closer to the body than the port vortex (the vortex on the blowing-nozzle-side). With blowing on the port side, the vortices are observed to switch their relative positions with the blowing-nozzle-side vortex assuming the low vortex position and the vortex on the opposite side assuming the high vortex position. This switch in the relative vortex positions is expected to

manifest itself as a change in the magnitude in the sectional side force.

The effectiveness of blowing from a given nozzle exit geometry is determined from the change in the sectional side force with blowing for each nozzle relative to its baseline condition. Thus, ΔC_y that is the difference of the sectional side force with blowing from the sectional side force with no blowing was calculated. The magnitude of ΔC_y is a measure of the relative blowing effectiveness, while a negative ΔC_y is indicative of a reversal in the direction of the side force due to the effect of blowing. Figure 8 shows the incremental sec-

tional side forces plotted against the mean geometric center of the nozzle exit orifice $\bar{y}/d$ over the range of angles of attack tested. For the lowest angle of attack tested, $\alpha = 40$ deg, the effect of blowing from the different nozzle exit geometries is seen to be small. For the 50-deg angle-of-attack case, the incremental sectional side forces are larger in magnitude, and there is a noticeable effect of the nozzle exit geometry. Observing the data of rows 2 and 3, a lower positioned exit geometry is observed to be more effective with blowing than a higher positioned nozzle exit. For $\alpha = 60$ deg, there was an even larger contrast observed due to the change in mean geometric height. However, for this single nozzle configuration at the higher angles of attack, $\alpha = 50$ and 60 deg, the trend towards larger $|\Delta C_y|$ as the mean geometric height is reduced is not monotonic. The irregular behavior is a consequence of the large asymmetry in the baseline flow; thus the effect of the baseline vortex flow on the effectiveness of blowing from different nozzle exit geometries was next examined.

Double Nozzle Configuration

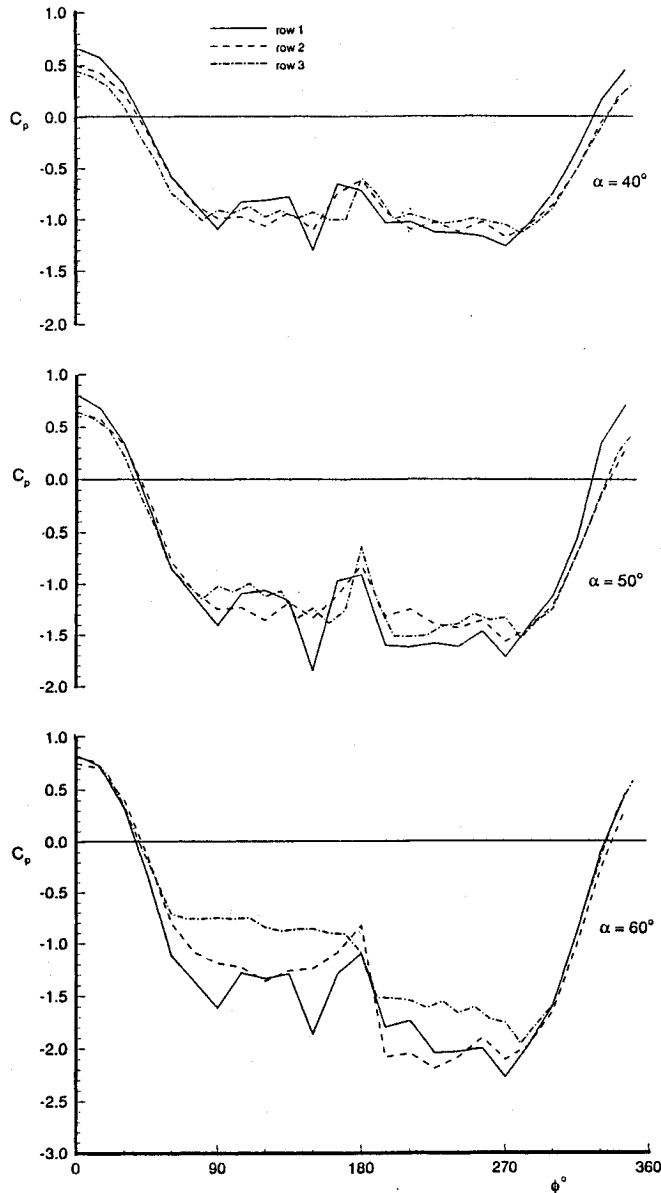The double nozzle configuration was initially tested with the blowing nozzles sealed, i.e., $C_\mu = 0$. Figure 9 shows the double nozzle configuration pressure distributions for blowing nozzle 5, over the range of angles of attack investigated. This data is representative of the trends observed for the no-blowing cases with the other four blowing nozzles. While varying degrees of vortex asymmetry were observed, as α is changed, the baseline vortex system exhibits less asymmetry than the single nozzle configuration data presented in Fig. 5. When the model was positioned at 40-deg angle of attack, the vortices on the leeside of the model were quite symmetric. As the angle of attack increased through 50–60 deg, the degree of vortex asymmetry is observed to increase, as inferred from the more negative C_p in the range 180 deg $\leq \phi \leq$ 270 deg. The vortex on the blowing-nozzle-side (port side) of the model assumed the high vortex position, while the opposite vortex (starboard side) assumed the low vortex position. Again these no-blowing cases will be taken as the baseline test conditions for this portion of the research.

Figure 10 shows the sectional side force plotted against $\bar{y}/d$ for the baseline test cases. As expected from the above C_p distributions, for each blowing nozzle, that is a fixed $\bar{y}/d$, the magnitude of the sectional side force increased with increasing angle of attack. This confirmed the increase in the vortex asymmetry with increasing angle of attack. At each

Fig. 9   Pressure coefficient for double nozzle configuration baseline condition for nozzle 5, $C_\mu = 0.0$.
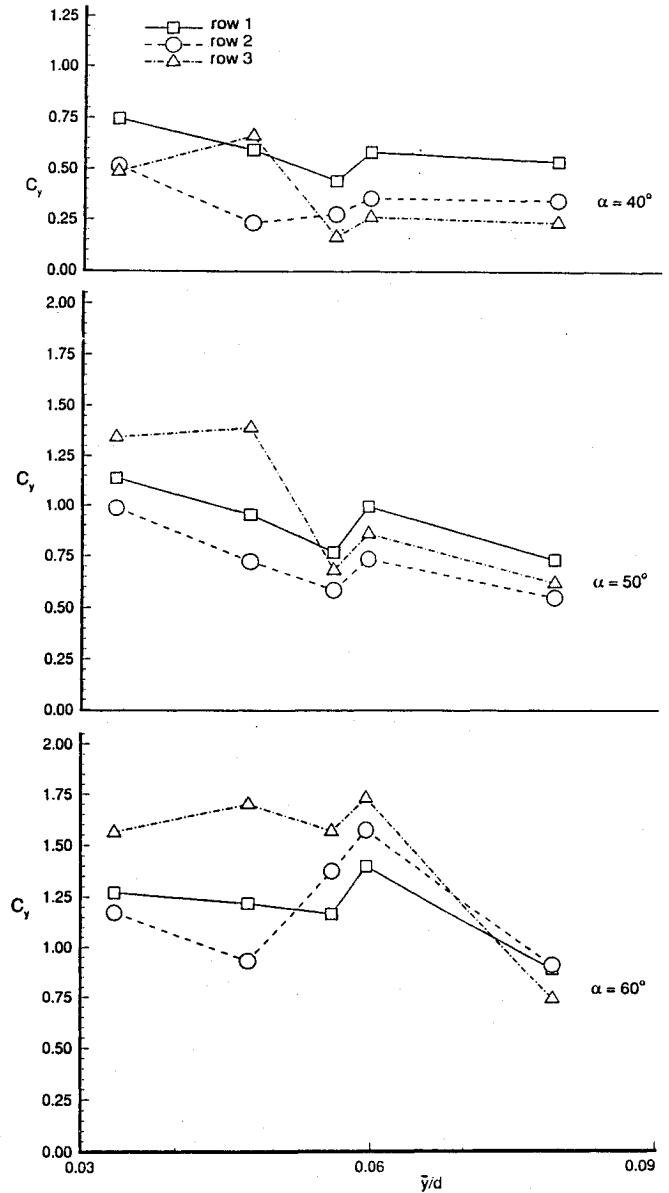
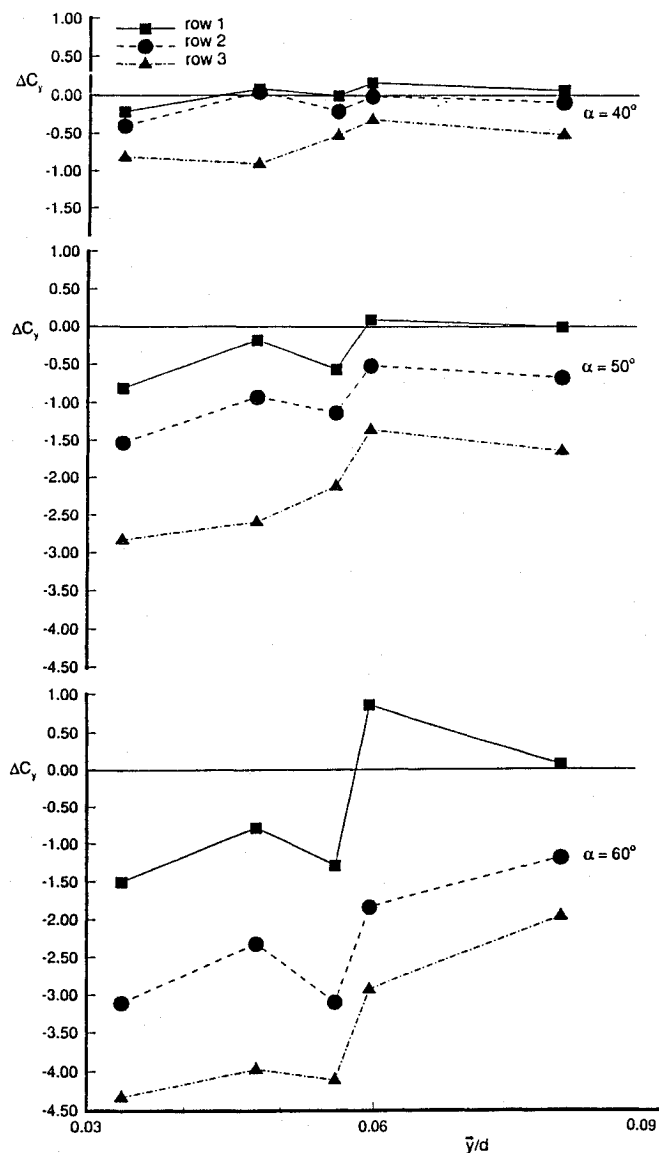Fig. 10   Sectional side force coefficient for double nozzle configuration baseline condition, $C_\mu = 0.0$.

Fig. 11 Incremental sectional side force coefficient for double nozzle configuration baseline condition, $C_\mu = 0.4$.

angle of attack, relatively small variations in C_y were observed with changing $\bar{y}/d$. This result indicated that the effects of interchanging the blowing nozzles were minimal, and that within the machining accuracy of the different blowing nozzles, the baseline conditions were the same for all five blowing nozzles. It is also relevant to point out that the baseline sectional side forces for the double nozzle configuration are smaller in magnitude than for the single nozzle configuration (Fig. 6). (Note that the range of the vertical axis is smaller for the double nozzle configuration than for the single nozzle configuration).

The effectiveness of blowing from the different nozzle exit geometries is examined in Fig. 11, where the incremental sectional side force is plotted against the mean geometric height. At $\alpha = 40$ deg, the direction of the sectional side force is reversed as a consequence of the blowing, but there is little change in ΔC_y at a given row as the nozzle exit geometry is varied. At the intermediate angle of attack ($\alpha = 50$ deg) there is a more marked variation in ΔC_y. The largest incremental sectional side force was observed for the three blowing nozzles, 1–3, for which the mean geometric center was closest to the surface. These nozzles are the semielliptic nozzle exit with horizontal major axis, nozzle 1, the semicircular exit, nozzle 2, and the elliptic nozzle exit, nozzle 3. The

other two nozzles, 4 and 5, which had mean geometric centers farther away from the surface, were not as effective as the former set of nozzles. These data at $\alpha = 50$ deg show that there is a definite trend towards larger $|\Delta C_y|$ as the mean geometric height is reduced. It must, however, be noted (Table 1) that the effects of changing the nozzle exit width are also evident in Fig. 11. The effect of the nozzle exit width is demonstrated by comparing blowing nozzles 3 and 4, which have nearly identical mean geometric centers, but in which the former nozzle is wider than the latter blowing nozzle. The wider nozzle exit is apparently more beneficial in terms of the blowing effectiveness. The blowing effectiveness from the different nozzle exit geometries is more clearly marked at $\alpha = 60$ deg. Overall, these results for the double nozzle configuration suggest that a low, broad nozzle exit geometry is more effective for blowing than a high, narrow nozzle exit.

Concluding Remarks

An experimental study has been conducted to examine the effect of the nozzle exit geometry on the effectiveness of aft blowing as a forebody vortex control technique. A 3.0-tangent caliber ogive model was tested at subsonic velocities and a Reynolds number of 8.4×10^4 based on the model base diameter. The effect of the nozzle exit geometry was studied using asymmetric blowing from five different nozzle exit cross sections. A single and a double nozzle configuration were tested to determine the influence of the baseline vortex system.

The following conclusions are drawn from this study:

1) For both configurations at moderate-to-high angles of attack, the effectiveness of aft blowing is influenced by both the width and height of the nozzle exit geometry. The results obtained indicate that a broad, low cross-sectional exit is more effective for forebody vortex control than a narrow, high cross section.

2) The degree of symmetry of the baseline vortex flow, that is flow without blowing, is also found to be a moderating effect on the blowing effectiveness.

These findings are encouraging and warrant further research of the effects of the magnitude of blowing, the effects of sideslip flow, and other nozzle exit geometries.

References

[1]Ericsson, L. E., "Control of Forebody Flow Asymmetry—A Critical Review," Proceedings of the AIAA Atmospheric Flight Mechanics Conference (Portland, OR), AIAA, Washington, DC, 1990, pp. 326–348.

[2]Moskovitz, C. A., Hall, R. M., and DeJarnette, F. R., "Effects of Surface Perturbations on the Asymmetric Vortex Flow over a Slender Body," AIAA Paper 88-0483, Jan. 1988.

[3]Moskovitz, C. A., Hall, R. M., and DeJarnette, F. R., "Effects of Nose Bluntness, Roughness, and Surface Perturbations on the Asymmetric Flow Past Slender Bodies at Large Angles of Attack," AIAA Paper 89-2236, July 1989; see also Moskovitz, C. A., Hall, R. M., and DeJarnette, F. R., "Combined Effects of Nose Bluntness and Surface Perturbations on Asymmetric Flow Past Slender Bodies," Journal of Aircraft, Vol. 27, No. 5, 1990, pp. 909, 910.

[4]Moskovitz, C. A., Hall, R. M., and DeJarnette, F. R., "Experimental Investigation of a New Device to Control the Asymmetric Flowfield on Forebodies at Large Angles of Attack," AIAA Paper 90-0069, Jan. 1990; see also Moskovitz, C. A., Hall, R. M., and

DeJarnette, F. R., "New Device for Controlling the Asymmetric Flowfields on Forebodies at Large Alpha," *Journal of Aircraft*, Vol. 28, No. 4, 1991, pp. 456–462.

[5]Ng, T. T., and Malcolm, G. N., "Aerodynamic Control Using Forebody Vortex Control," *Proceedings of the High-Angle-of-Attack Technology Conference*, Vol. 1, 1990, pp. 507–532 (NASA CP-3149).

[6]Ng, T. T., and Malcolm, G. N., "Aerodynamic Control Using Forebody Blowing and Suction," AIAA Paper 91-0619, Jan. 1991.

[7]Ng, T. T., Ong, L. Y., Suarez, C. J., and Malcolm, G. N., "Wing Rock Suppression Using Forebody Vortex Control," *Proceedings of the AIAA 9th Applied Aerodynamics Conference* (Baltimore, MD), AIAA, Washington, DC, 1991, pp. 198–211.

[8]Gittner, N. M., and Chokani, N., "An Experimental Study of the Effects of Aft Blowing on a 3.0 Caliber Tangent Ogive Body at High Angles of Attack," *Proceedings of the AIAA 9th Applied Aerodynamics Conference* (Baltimore, MD), AIAA, Washington, DC, 1991, pp. 390–399.

[9]Gittner, N. M., "An Experimental Study of the Effects of Aft Blowing on a 3.0 Caliber Tangent Ogive Body at High Angles of Attack," M.S. Thesis, North Carolina State Univ., Raleigh, NC, March 1992.